

Characterizing gas flow from aerosol particle injectors

Daniel A. Horke,^{1,2,*} Nils Roth,^{1,3} Lena Worbs,¹ and Jochen Küpper^{1,2,3}

¹Center for Free-Electron Laser Science, DESY, Notkestrasse 85, 22607 Hamburg, Germany

²The Hamburg Center for Ultrafast Imaging, University of Hamburg, Luruper Chaussee 149, 22761 Hamburg, Germany

³Department of Physics, University of Hamburg, Luruper Chaussee 149, 22761 Hamburg, Germany

(Dated: September 29, 2016)

A novel methodology for measuring gas flow from small orifices or nozzles into vacuum is presented. It utilizes a high-intensity femtosecond laser pulse to create a plasma within the gas plume produced by the nozzle, which is imaged by a microscope. Calibration of the imaging system at known chamber pressures allows for the extraction of absolute number densities, and we show detection down to helium densities of $4 \times 10^{16} \text{ cm}^{-3}$ with a spatial resolution of a few micrometer. The technique is used to characterize the gas flow from a convergent-nozzle aerosol injector as used in single-particle diffractive imaging experiments at free-electron laser sources. Based on the measured gas-density profile we estimate the scattering background signal under typical operating conditions of single-particle imaging experiments and estimate that fewer than 50 photons per shot can be expected on the typical detector of such an experiment.

I. INTRODUCTION

The advances of x-ray free-electron lasers (XFELs), which provide intense and short pulses of coherent x-rays, open up new possibilities for imaging of aerosolized particles, and even individual molecules, with atomic spatial resolution [1–4]. As experiments can be conducted completely in the gas-phase and do not require sample immobilization, e. g., cryogenic freezing, XFELs furthermore provide unprecedented capabilities for capturing ultrafast dynamics of isolated systems with femtosecond temporal and picometer spatial resolution [4–6]. This is enabled by the short and intense x-ray pulses available at these facilities, which typically provide pulses with $\sim 1 \text{ mJ}$ pulse energy, $\sim 10 \text{ fs}$ pulse duration, and $\sim 100 \text{ pm}$ wavelength. This allows the imaging methodology to outrun radiation damage effects in the *diffraction before destruction* mechanism [7–10]. Combining many diffraction patterns from reproducible isolated aerosol targets imaged at random orientations should allow one to reconstruct the three-dimensional, atomically resolved structure [11, 12]. In recent years full 3D reconstruction has been demonstrated and the achieved resolution continuously improved [13–16].

The advent of these new possibilities for imaging isolated systems *in vacuo* has prompted the development and improvement of techniques for injecting samples into the interaction region. Using gas-dynamic virtual nozzles (GDVNs) [17] for producing focussed liquid jets enabled the serial femtosecond crystallography (SFX) methodology [18, 19], allowing the reconstruction of sub-nanometer-resolution structures from micrometer sized crystals [18, 20]. Aerodynamic lenses [1, 21] and convergent-nozzle injectors [22] are widely used injection techniques to produce focused or collimated streams of

nano- or micrometer sized particles. They fundamentally rely on a gas flow that interacts with the particles of interest and, through shear and drag forces, produces the desired stream of particles. Typically, helium is used for its relatively small x-ray scattering cross-section. However, since the helium gas density at the interaction point is still many orders of magnitude higher than the sample density, scattering from the focusing gas can make a significant contribution to the recorded background scattering [2, 23, 24]. In order to account for this background and to make quantitative predictions and background calibrations, therefore, requires knowledge of the gas density at the interaction point, typically located a few hundred micrometers below the injector tip [22].

Here, we present a methodology that allows the spatially resolved measurement of gas densities down to $\sim 4 \times 10^{16} \text{ cm}^{-3}$ with high spatial and, potentially, temporal resolution. This is achieved by using a high-intensity femtosecond laser pulse to create a plasma within the gas-stream, which is then imaged by a microscope objective and camera. The observed intensity of the plasma depends on the local gas pressure in the laser focus. By calibrating the plasma formation and imaging system to known helium pressures, this method allows us to create spatial maps of the gas flow from an injector tip. Compared to previous methods, this approach provides a higher sensitivity, allowing the detection of one order of magnitude lower gas pressures, and it does not rely on interferometric measurements prone to mechanical instabilities [25, 26]. In particular, we characterize a convergent nozzle injector [22] under typical operation conditions for XFEL single particle diffractive imaging experiments. Based on the measured gas-density distribution, the x-ray scattering signal expected from this helium background at typical operating parameters of currently available XFEL endstations is calculated.

* daniel.horke@cfel.de;
https://www.controlled-molecule-imaging.org

II. EXPERIMENTAL METHOD

To assess the local gas density at the tip of an aerosol injector we crossed the gas stream with a focused femtosecond laser beam of sufficient intensity to produce a plasma inside the gas-stream. The bright visible glow of this plasma was recorded on a camera. The intensity depended on the laser intensity and the gas density in the interaction volume. By calibrating the imaging system at known gas densities, this allowed us to build up a high-resolution spatial map of local gas-densities produced by the injector tip.

A simple sketch of the vacuum and imaging system is shown in Figure 1. The vacuum system consisted of two differentially pumped chambers, connected only through the injector tip. The upper chamber (i. e., upstream of the injector) contained a capacitive pressure gauge (Pfeiffer Vacuum CMR361) with an absolute accuracy of 0.2% independent of gas type, a high-precision leak valve connected to a high-purity helium supply and a connection

to a roughing pump, with the pumping speed controllable through a needle valve. This setup allowed us to maintain a constant pressure during operation of the injector by matching the helium flow into the upper chamber to the gas transmission through the injector aperture. This chamber mimicked the typical nebulization chamber in single-particle imaging experiments. At the bottom of this upper chamber and mounted on a 6 mm outer diameter stainless steel tube was the injector tip (30° convergence angle, orifice $111\ \mu\text{m}$) [22], located within the main vacuum chamber as shown in Figure 1. This chamber was evacuated by a turbomolecular pump (Pfeiffer Vacuum HiPace 80) and the pressure was monitored through a full-range pressure gauge (Pfeiffer Vacuum PKR361). The laser-matter interaction was imaged through a standard vacuum viewport with a $10\times$ long working-distance microscope objective (Edmund Optics) that produced an image on a high-sensitivity CMOS camera (Thorlabs DCC3240M, 10 bit monochrome). Residual stray infrared light from the femtosecond laser was blocked using two shortpass filters (Thorlabs FESH0700, $\text{OD} > 5$ for $\lambda > 700\ \text{nm}$) mounted between the objective and the camera and stray light was reduced by mechanically enclosing the optical path. The entire imaging system (objective, filters, camera) was mounted on a three-dimensional translation stage.

The laser passed through the interaction chamber perpendicular to both, the gas-stream and the imaging axis, as indicated by the red cross in Figure 1. It consisted of pulses from an amplified Ti:Sapphire laser system (Spectra Physics Spitfire ACE) centered around $800\ \text{nm}$, running at $1\ \text{kHz}$ repetition rate, and producing $40\ \text{fs}$ pulses with $0.7\ \text{mJ}$ per pulse used in the current experiment. The laser was focused into the interaction region with a $f = 300\ \text{mm}$ plano-convex lens, producing a focal spot size of $50\ \mu\text{m}$ (4σ) with a nominal Rayleigh range of $\sim 2.5\ \text{mm}$ and a peak intensity of $8.9 \times 10^{14}\ \text{W}/\text{cm}^2$. The focusing lens was placed on a 3D translation stage to allow translation of the laser focus in space to ensure overlap with the gas stream within the Rayleigh range and to allow probing of the local gas densities at different distances from the injector nozzle.

The imaging system was calibrated by recording the plasma-glow intensity when flooding the chamber to a known helium pressure; details are given in the supplementary information. To collect data from the injector produced plasma, the injector tip was installed in the center of the chamber and the upper chamber was pressurized with helium as discussed above. The horizontal laser-injector overlap, i. e., along the imaging axis, was optimized to produce the brightest plasma. Then the vertical position of the laser was adjusted by translating the focusing lens, such that it passed just below the injector tip. The laser focus was translated downwards in steps of $12.5\ \mu\text{m}$ and at every point 20 frames were collected on the camera. The exposure time was adjusted such that the plasma was clearly visible but no saturation occurs. During the subsequent data analysis the images collected

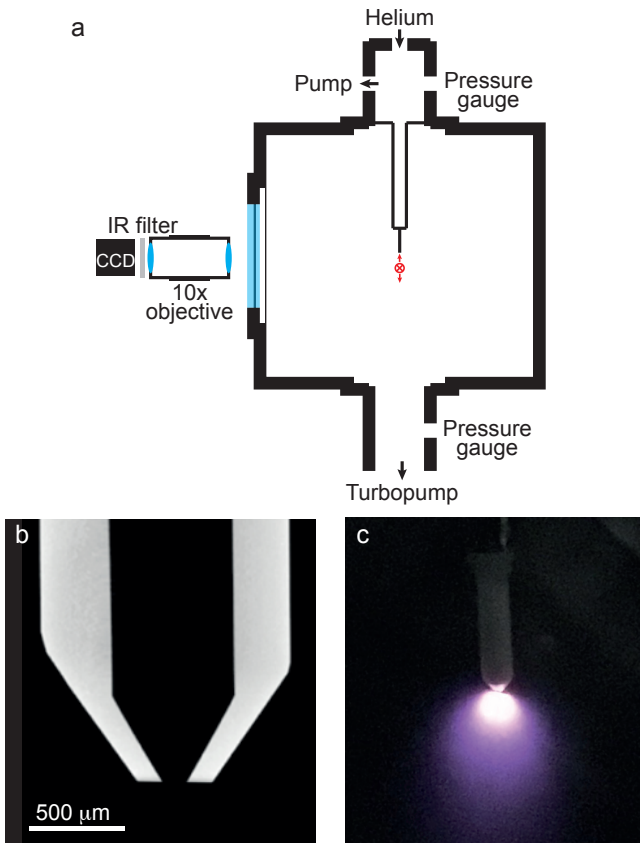


FIG. 1. a) Sketch of the experimental setup and imaging system. The laser propagates out of the plane of the page (indicated by the red cross) and can be translated in height using a motorized translation stage. b) X-ray tomogram of a convergent injector tip, c.f. reference 22. c) Picture of the operating injector in the vacuum chamber, showing the produced plasma during helium injection (recorded with a standard mobile phone camera).

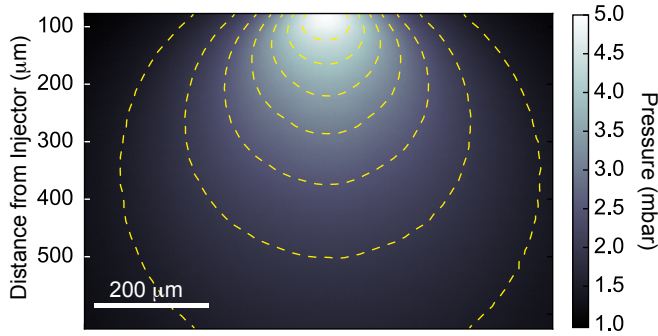


FIG. 2. Pressure map recorded below the tip of a convergent injector nozzle for an upstream pressure of 800 mbar helium. Dashed yellow lines indicate isobars from 1.5 to 4.5 mbar in 0.5 mbar intervals.

at the same position were averaged and scaled by exposure time. Then all images from a single upstream pressure were combined, keeping for every pixel the maximum intensity that occurs in one of the images. This “max intensity stack” approach was chosen because the produced plasma continues to glow for an appreciable time even after the laser pulse has past through the sample. As the gas is moving rapidly away from the nozzle – due to choked flow conditions the speed is probably close 1000 m/s – this led to intensity on the camera below the interaction point with the laser, as can clearly be seen on the photograph in Figure 1 b. Averaging collected images from different positions, therefore, would have overexposed the lower part of the image. The pressure for every pixel was retrieved by comparison with the calibration measurements.

III. RESULTS AND DISCUSSION

The measured pressure distribution from a convergent nozzle tip operated with 800 mbar of upstream helium is shown in Figure 2. Similar measurements for upstream pressures of 300 mbar and 500 mbar are shown in the supplementary materials. During the measurement the pressure in the main chamber was maintained below 2×10^{-2} mbar, ensuring choked-flow-conditions through the orifice. The topmost measurement was taken around 80 μm below the tip; moving the laser further up leads to clipping of the beam, and potentially damage, on the ceramic tip. At distances $\gtrsim 600$ μm below the tip the pressure had fallen such that no plasma was observed. The gas pressure was found to decrease dramatically with increasing distance from the injector tip, as expected. Due to the acceleration of gas inside the orifice, initially some propensity for the helium to continue along the axial direction is observed, rather than radially isotropic diffusion, resulting in the non-spherical pressure distribution measured. Under typical operating conditions for single-particle diffractive imaging experiments, the interaction region, that is, the crossing point of the x-ray

beam with the particle stream, is located ~ 300 μm below the injector tip. At this position the pressure has already dropped considerably and, for the measurements of 800 mbar upstream pressure (Figure 2) is on the order of 3 mbar.

To quantify the spatial resolution in the produced images we differentiate between the resolution within the imaging plane, i. e., within the plane of laser illumination, and the resolution parallel to the camera surface. The latter is limited only by the imaging system employed. For the current setup a single pixel corresponds to 0.86 μm , however due to aberrations and mechanical instabilities we estimate the resolution in this plane to be on the order of 2 μm . In the direction perpendicular to the imaging plane, the resolution is not only limited by the depth of focus of the imaging system, but also by the focal spot size of the illuminating laser, which is around 50 μm (4σ) for the data shown. This is, however, still significantly smaller than the orifice size of the injector, allowing us to image essentially the central slice through the (radially symmetric) pressure distribution.

Helium pressure profiles along both the axial and radial directions are shown in Figure 3, where the measured pressure has been converted into an absolute number density assuming ideal gas behavior. Figure 3(a) shows the axial density distribution along the center line of the injector as a function of distance from the tip, for different upstream pressures. The pressure decreases rapidly with distance from the injector, and exhibits approximately a $1/r^3$ dependence, which is shown by the dashed lines in Figure 3 a, as would be expected for an isotropic radial diffusion in 3D. For the production of focused nanoparticle beams the pressure upstream of the injector is typically in the range of 200–500 mbar, while the particle focus – and hence interaction point – is located a few hundred micrometer downstream the nozzle [22]. Therefore, the corresponding number densities at the interaction point are typically on the order of $5 \times 10^{16} \text{ cm}^{-3}$. Radial profiles of the helium number density are shown in Figure 3 b, measured at various distances below the injector tip for an upstream pressure of 800 mbar; profiles for further upstream pressures are shown in the supplementary information. These clearly show that the initially narrow gas plume spreads out radially, leading to a rapid decrease in the absolute density along the center line.

To assess the total scattering signal that can be expected from helium in XFEL based diffraction experiments, one has to take into account not only the interaction point itself, but due to the large Rayleigh length of the XFEL beam, typically several millimeters, one should take into account the full extend of the helium “cloud” along the x-ray beam, the extend of which is visible from the radial profiles in Figure 3 b. From our spatially resolved measurements we can assess the average helium density encountered by the XFEL pulse as it travels through the helium cloud, and for 500 mbar upstream pressure this is $\sim 3.6 \times 10^{16} \text{ cm}^{-3}$, corresponding to the average helium density 300 μm below the injector tip as measured within

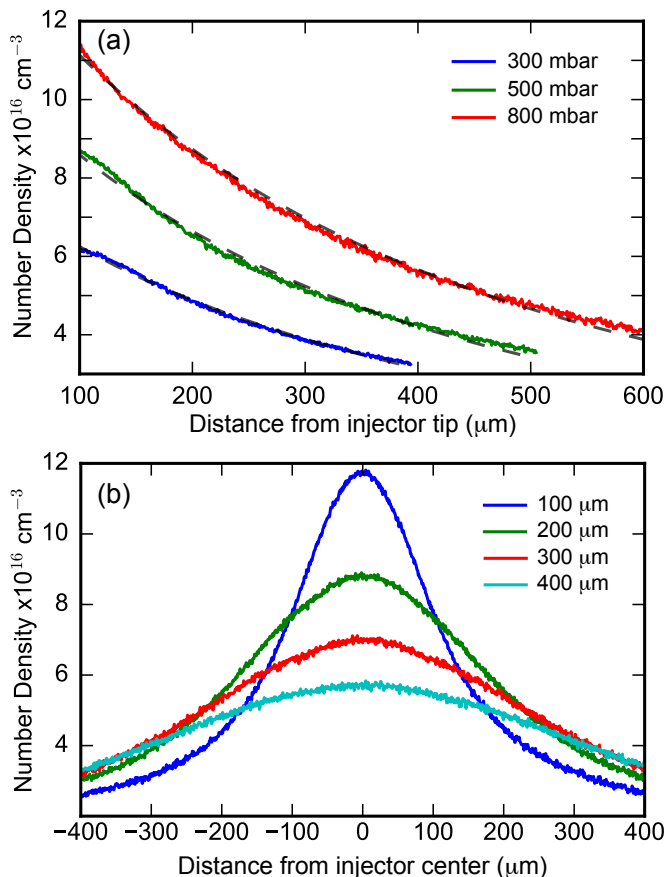


FIG. 3. Gas density profiles. (a) Axial profile of the number density along the center of the injector as a function of distance from the tip, shown for three different upstream helium pressures. Dashed lines correspond to a $1/r^3$ fit. (b) Radial profiles of the number density across the generated plume for 800 mbar upstream pressure, at three different distances from the injector tip.

our field of view. Considering the known helium cross sections for elastic (Rayleigh) and inelastic (Compton) scattering, and typical operating conditions for the CXI endstation at the Linear Coherent Light Source (LCLS), e.g., 10 keV photon energy and 10^{11} photons per pulse, we expect a total of ~ 500 scattered x-ray photons per shot due to the helium background gas. Considering an isotropic scattering distribution and a detector opening angle of 60° , this corresponds to ~ 40 photons per shot on the detector. We furthermore note that the majority of these photons ($> 70\%$) originate from inelastic scattering processes, and can thus potentially be discriminated

against by an energy-resolving detector [27].

IV. CONCLUSION

We present a robust and sensitive approach for measuring the spatial distribution of gas flows from nozzles into vacuum. Calibration at known pressures allows the determination of absolute pressures and number densities with high spatial resolution. With the current setup the minimum detectable density is on the order of 10^{16} cm^{-3} , around one order of magnitude smaller than with interferometric approaches [25, 26]. The spatial resolution within the imaging plane is around $2 \mu\text{m}$, perpendicular to the imaging plane it is limited by the laser spot size of $50 \mu\text{m}$ (4σ). We also note that this methodology can be further extended to measurements in the time domain, due to the inherently pulsed nature of the laser illumination.

We used this approach to assess the gas flow from a convergent nozzle injector [22] typically used for single-particle diffractive imaging experiments. We found that at typical operating conditions the gas density in the interaction region is on the order $5 \times 10^{16} \text{ cm}^{-3}$. By evaluating the average gas density encountered by an x-ray pulse as it travels through the gas plume we estimate that fewer than 500 photons will be scattered by the helium. This number could be further reduced by increasing the distance between the injector tip and the interaction region, which could be facilitated through the use of shallower convergence angles within the injector [22]. Further approaches to reduce the incoherent scattering from helium could incorporate inhomogeneous electric fields to deflect particles of interest out of the helium plume [28], as has been demonstrated for single molecule scattering experiments at LCLS utilizing supersonic molecular beams [2].

ACKNOWLEDGMENTS

We gratefully acknowledge support by Salah Awel with the aerosol injector tips and Christian Kruse in an early stage of the experiment.

In addition to DESY, this work has been supported by the excellence cluster “The Hamburg Center for Ultrafast Imaging – Structure, Dynamics and Control of Matter at the Atomic Scale” of the Deutsche Forschungsgemeinschaft (CUI, DFG-EXC1074) and by the European Research Council through the Consolidator Grant COMOTION (ERC-614507).

[1] Michael J Bogan, W Henry Benner, Sebastien Boutet, Urs Rohner, Matthias Frank, Anton Barty, M. Marvin Seibert, Filipe Maia, Stefano Marchesini, Saša Bajt, Bruce Woods, Vincent Riot, Stefan P Hau-Riege, Martin Svenda, Erik Marklund, Eberhard Spiller, Janos Hajdu, and

Henry N Chapman, “Single particle x-ray diffractive imaging,” *Nano Letters* **8**, 310–316 (2008).

[2] Jochen Küpper, Stephan Stern, Lotte Holmegaard, Frank Filsinger, Arnaud Rouzée, Artem Rudenko, Per Johnsson, Andrew V. Martin, Marcus Adolph, Andrew Aquila, Saša

- Bajt, Anton Barty, Christoph Bostedt, John Bozek, Carl Caleman, Ryan Coffee, Nicola Coppola, Tjark Delmas, Sascha Epp, Benjamin Erk, Lutz Foucar, Tais Gorkhover, Lars Gumprecht, Andreas Hartmann, Robert Hartmann, Günter Hauser, Peter Holl, Andre Hömke, Nils Kimmel, Faton Krasniqi, Kai-Uwe Kühnel, Jochen Maurer, Marc Messerschmidt, Robert Moshhammer, Christian Reich, Benedikt Rudek, Robin Santra, Ilme Schlichting, Carlo Schmidt, Sebastian Schorb, Joachim Schulz, Heike Soltau, John C. H. Spence, Dmitri Starodub, Lothar Strüder, Jan Thøgersen, Marc J. J. Vrakking, Georg Weidenspointner, Thomas A. White, Cornelia Wunderer, Gerard Meijer, Joachim Ullrich, Henrik Stapelfeldt, Daniel Rolles, and Henry N. Chapman, “X-ray diffraction from isolated and strongly aligned gas-phase molecules with a free-electron laser,” *Phys. Rev. Lett.* **112**, 083002 (2014), arXiv:1307.4577 [physics].
- [3] John C H Spence and Henry N Chapman, “The birth of a new field,” *Phil. Trans. R. Soc. B* **369**, 20130309–20130309 (2014).
- [4] Anton Barty, Jochen Küpper, and Henry N Chapman, “Molecular imaging using x-ray free-electron lasers,” *Annu. Rev. Phys. Chem.* **64**, 415–435 (2013).
- [5] Kanupriya Pande, Christopher D. M. Hutchison, Gerrit Groenhof, Andy Aquila, Josef S. Robinson, Jason Tenboer, Shibom Basu, Sébastien Boutet, Daniel P. DePonte, Mengning Liang, Thomas A. White, Nadia A. Zatsepin, Oleksandr Yefanov, Dmitry Morozov, Dominik Oberthuer, Cornelius Gati, Ganesh Subramanian, Daniel James, Yun Zhao, Jake Koralek, Jennifer Brayshaw, Christopher Kupitz, Chelsie Conrad, Shatabdi Roy-Chowdhury, Jesse D. Coe, Markus Metz, Paulraj Lourdu Xavier, Thomas D. Grant, Jason E. Koglin, Gihan Ketawala, Raimund Fromme, Vukica Šrajer, Robert Henning, John C. H. Spence, Abbas Ourmazd, Peter Schwander, Uwe Weierstall, Matthias Frank, Petra Fromme, Anton Barty, Henry N. Chapman, Keith Moffat, Jasper J. van Thor, and Marius Schmidt, “Femtosecond structural dynamics drives the trans/cis isomerization in photoactive yellow protein,” *Science* **352**, 725–729 (2016).
- [6] Tais Gorkhover, Sebastian Schorb, Ryan Coffee, Marcus Adolph, Lutz Foucar, Daniela Rupp, Andrew Aquila, John D. Bozek, Sascha W. Epp, Benjamin Erk, Lars Gumprecht, Lotte Holmegaard, Andreas Hartmann, Robert Hartmann, Günter Hauser, Peter Holl, Andre Hömke, Nils Kimmel, Kai-Uwe Kühnel, Per Johnsson, Marc Messerschmidt, Christian Reich, Arnaud Rouzeé, Benedikt Rudek, Carlo Schmidt, Joachim Schulz, Heike Soltau, Stephan Stern, Georg Weidenspointner, Bill White, Jochen Küpper, Lothar Strüder, Ilme Schlichting, Joachim Ullrich, Daniel Rolles, Artem Rudenko, Thomas Möller, and Christoph Bostedt, “Femtosecond and nanometre visualization of structural dynamics in superheated nanoparticles,” *Nat. Photon.* **10**, 93–97 (2016).
- [7] R. Neutze, R. Wouts, D. van der Spoel, E. Weckert, and J. Hajdu, “Potential for biomolecular imaging with femtosecond X-ray pulses,” *Nature* **406**, 752–757 (2000).
- [8] B Ziaja, H N Chapman, R Fäustlin, S Hau-Riege, Z Jurek, A V Martin, S Toleikis, F Wang, E Weckert, and R Santra, “Limitations of coherent diffractive imaging of single objects due to their damage by intense x-ray radiation,” *New J. Phys.* **14**, 115015 (2012).
- [9] U. Lorenz, N. M. Kabachnik, E. Weckert, and I. A. Vartanyants, “Impact of ultrafast electronic damage in single-particle x-ray imaging experiments,” *Phys. Rev. E* **86**, 051911 (2012).
- [10] Karol Nass, Lutz Foucar, Thomas R. M. Barends, Elisabeth Hartmann, Sabine Botha, Robert L. Shoeman, R. Bruce Doak, Roberto Alonso-Mori, Andrew Aquila, Saša Bajt, Anton Barty, Richard Bean, Kenneth R. Beyerlein, Maike Bublitz, Nikolaj Drachmann, Jonas Gregersen, H. Olof Jönsson, Wolfgang Kabsch, Stephan Kassemeyer, Jason E. Koglin, Michael Krumrey, Daniel Mattle, Marc Messerschmidt, Poul Nissen, Linda Reinhard, Oleg Sitsel, Dimosthenis Sokaras, Garth J. Williams, Stefan Hau-Riege, Nicusor Timneanu, Carl Caleman, Henry N. Chapman, Sébastien Boutet, and Ilme Schlichting, “Indications of radiation damage in ferredoxin microcrystals using high-intensity x-fel beams,” *J. Synchrotron Rad.* **22**, 225–238 (2015).
- [11] Magnus Bergh, Gösta Huldt, Nicusor Timneanu, Filipe R. N. C. Maia, and Janos Hajdu, “Feasibility of imaging living cells at subnanometer resolutions by ultrafast x-ray diffraction,” *Quarterly Reviews of Biophysics* **41**, 181–204 (2008).
- [12] R Fung, A M Hanna, O Vendrell, S Ramakrishna, T Seideman, R Santra, and A Ourmazd, “Dynamics from noisy data with extreme timing uncertainty,” *Nature* **532**, 471–475 (2016).
- [13] M Marvin Seibert, Tomas Ekeberg, Filipe R N C Maia, Martin Svenda, Jakob Andreasson, Olof Jönsson, Duško Odić, Bianca Iwan, Andrea Rocker, Daniel Westphal, Max Hantke, Daniel P Deponte, Anton Barty, Joachim Schulz, Lars Gumprecht, Nicola Coppola, Andrew Aquila, Mengning Liang, Thomas A White, Andrew Martin, Carl Caleman, Stephan Stern, Chantal Abergel, Virginie Seltzer, Jean-Michel Claverie, Christoph Bostedt, John D Bozek, Sébastien Boutet, A Alan Miahnahri, Marc Messerschmidt, Jacek Krzywinski, Garth Williams, Keith O Hodgson, Michael J Bogan, Christina Y Hampton, Raymond G Sierra, Dmitri Starodub, Inger Andersson, Saša Bajt, Miriam Barthelmess, John C H Spence, Petra Fromme, Uwe Weierstall, Richard Kirian, Mark Hunter, R Bruce Doak, Stefano Marchesini, Stefan P Hau-Riege, Matthias Frank, Robert L Shoeman, Lukas Lomb, Sascha W Epp, Robert Hartmann, Daniel Rolles, Artem Rudenko, Carlo Schmidt, Lutz Foucar, Nils Kimmel, Peter Holl, Benedikt Rudek, Benjamin Erk, André Hömke, Christian Reich, Daniel Pietschner, Georg Weidenspointner, Lothar Strüder, Günter Hauser, Hubert Gorke, Joachim Ullrich, Ilme Schlichting, Sven Herrmann, Gerhard Schaller, Florian Schopper, Heike Soltau, Kai-Uwe Kühnel, Robert Andritschke, Claus-Dieter Schröter, Faton Krasniqi, Mario Bott, Sebastian Schorb, Daniela Rupp, Marcus Adolph, Tais Gorkhover, Helmut Hirsemann, Guillaume Potdevin, Heinz Graafsma, Björn Nilsson, Henry N Chapman, and Janos Hajdu, “Single mimivirus particles intercepted and imaged with an x-ray laser,” *Nature* **470**, 78 (2011).
- [14] Rui Xu, Huaidong Jiang, Changyong Song, Jose A Rodriguez, Zhifeng Huang, Chien-Chun Chen, Daewoong Nam, Jaehyun Park, Marcus Gallagher-Jones, Sangsoo Kim, Sunam Kim, Akihiro Suzuki, Yuki Takayama, Tomotaka Oroguchi, Yukio Takahashi, Jiadong Fan, Yunfei Zou, Takaki Hatsui, Yuichi Inubushi, Takashi Kameshima, Koji Yonekura, Kensuke Tono, Tadashi Togashi, Takahiro Sato, Masaki Yamamoto, Masayoshi Nakasako, Makina Yabashi, Tetsuya Ishikawa, and Jianwei Miao, “Single-shot three-

- dimensional structure determination of nanocrystals with femtosecond X-ray free-electron laser pulses,” *Nat. Commun.* **5**, 4061 (2014).
- [15] Max F Hantke, Dirk Hasse, MaiaFilipe R N C, Tomas Ekeberg, Katja John, Martin Svenda, N Duane Loh, Andrew V Martin, Nicusor Timneanu, LarssonDaniel S D, van der SchotGijs, Gunilla H Carlsson, Margareta Ingelman, Jakob Andreasson, Daniel Westphal, Mengning Liang, Francesco Stellato, Daniel P DePonte, Robert Hartmann, Nils Kimmel, Richard A Kirian, M Marvin Seibert, Kerstin Mühlig, Sebastian Schorb, Ken Ferguson, Christoph Bostedt, Sebastian Carron, John D Bozek, Daniel Rolles, Artem Rudenko, Sascha Epp, Henry N Chapman, Anton Barty, Janos Hajdu, and Inger Andersson, “High-throughput imaging of heterogeneous cell organelles with an x-ray laser,” *Nat. Photon.* **8**, 943–949 (2014).
- [16] Tomas Ekeberg, Martin Svenda, Chantal Abergel, Filipe R N C Maia, Virginie Seltzer, Jean-Michel Claverie, Max Hantke, Olof Jönsson, Carl Nettelblad, Gijs van der Schot, Mengning Liang, Daniel P Deponte, Anton Barty, M Marvin Seibert, Bianca Iwan, Inger Andersson, N Duane Loh, Andrew V Martin, Henry Chapman, Christoph Bostedt, John D Bozek, Ken R Ferguson, Jacek Krzywinski, Sascha W Epp, Daniel Rolles, Artem Rudenko, Robert Hartmann, Nils Kimmel, and Janos Hajdu, “Three-dimensional reconstruction of the giant mimivirus particle with an x-ray free-electron laser,” *Phys. Rev. Lett.* **114**, 098102 (2015).
- [17] D P DePonte, U Weierstall, K Schmidt, J Warner, D Starodub, J C H Spence, and R B Doak, “Gas dynamic virtual nozzle for generation of microscopic droplet streams,” *J. Phys. D Appl. Phys.* **41**, 195505 (2008).
- [18] Henry N Chapman, Petra Fromme, Anton Barty, Thomas A White, Richard A Kirian, Andrew Aquila, Mark S Hunter, Joachim Schulz, Daniel P Deponte, Uwe Weierstall, R Bruce Doak, Filipe R N C Maia, Andrew V Martin, Ilme Schlichting, Lukas Lomb, Nicola Coppola, Robert L Shoeman, Sascha W Epp, Robert Hartmann, Daniel Rolles, Artem Rudenko, Lutz Foucar, Nils Kimmel, Georg Weidenspointner, Peter Holl, Mengning Liang, Miriam Barthelmess, Carl Caleman, Sébastien Boutet, Michael J Bogan, Jacek Krzywinski, Christoph Bostedt, Saša Bajt, Lars Gumprecht, Benedikt Rudek, Benjamin Erk, Carlo Schmidt, André Hömke, Christian Reich, Daniel Pietschner, Lothar Strüder, Günter Hauser, Hubert Gorke, Joachim Ullrich, Sven Herrmann, Gerhard Schaller, Florian Schopper, Heike Soltau, Kai-Uwe Kühnel, Marc Messerschmidt, John D Bozek, Stefan P Hau-Riege, Matthias Frank, Christina Y Hampton, Raymond G Sierra, Dmitri Starodub, Garth J Williams, Janos Hajdu, Nicusor Timneanu, M Marvin Seibert, Jakob Andreasson, Andrea Rocker, Olof Jönsson, Martin Svenda, Stephan Stern, Karol Nass, Robert Andritschke, Claus-Dieter Schröter, Faton Krasniqi, Mario Bott, Kevin E Schmidt, Xiaoyu Wang, Ingo Grotjohann, James M Holton, Thomas R M Barends, Richard Neutze, Stefano Marchesini, Raimund Fromme, Sebastian Schorb, Daniela Rupp, Marcus Adolph, Tais Gorkhover, Inger Andersson, Helmut Hirsemann, Guillaume Potdevin, Heinz Graafsma, Björn Nilsson, and John C H Spence, “Femtosecond x-ray protein nanocrystallography,” *Nature* **470**, 73 (2011).
- [19] Ilme Schlichting, “Serial femtosecond crystallography: the first five years,” *IUCrJ* **2**, 246–255 (2015).
- [20] Kartik Ayyer, Oleksandr M Yefanov, Dominik Oberthür, Shatabdi Roy-Chowdhury, Lorenzo Galli, Valerio Mariani, Shibom Basu, Jesse Coe, Chelsie E Conrad, Raimund Fromme, Alexander Schaffer, Katerina Dörner, Daniel James, Christopher Kupitz, Markus Metz, Garrett Nelson, Paulraj Lourdu Xavier, Kenneth R Beyerlein, Marius Schmidt, Iosifina Sarrou, John C H Spence, Uwe Weierstall, Thomas A White, Jay-How Yang, Yun Zhao, Mengning Liang, Andrew Aquila, Mark S Hunter, Joseph S Robinson, Jason E Koglin, Sébastien Boutet, Petra Fromme, Anton Barty, and Henry N Chapman, “Macromolecular diffractive imaging using imperfect crystals,” *Nature* **530**, 202–206 (2016).
- [21] Peng Liu, Paul J Ziemann, David B Kittelson, and Peter H McMurry, “Generating particle beams of controlled dimensions and divergence: I. theory of particle motion in aerodynamic lenses and nozzle expansions,” *Aerosol Sci. Techn.* **22**, 293–313 (1995).
- [22] R. A. Kirian, S. Awel, N. Eckerskorn, H. Fleckenstein, M. Wiedorn, L. Adriano, S. Bajt, M. Barthelmess, R. Bean, K. R. Beyerlein, L. M. G. Chavas, M. Domaracky, M. Heymann, D. A. Horke, J. Knoska, M. Metz, A. Morgan, D. Oberthuer, N. Roth, T. Sato, P. L. Xavier, O. Yefanov, A. V. Rode, Jochen Küpper, and Henry N. Chapman, “Simple convergent-nozzle aerosol injector for single-particle diffractive imaging with x-ray free-electron lasers,” *Struct. Dyn.* **2**, 041717 (2015).
- [23] Stephan Stern, Lotte Holmegaard, Frank Filsinger, Arnaud Rouzee, Artem Rudenko, Per Johnsson, Andrew V. Martin, Anton Barty, Christoph Bostedt, John Bozek, Ryan Coffee, Sascha Epp, Benjamin Erk, Lutz Foucar, Robert Hartmann, Nils Kimmel, Kai-Uwe Kühnel, Jochen Maurer, Marc Messerschmidt, Benedikt Rudek, Dmitri Starodub, Jan Thøgersen, Georg Weidenspointner, Thomas A. White, Henrik Stapelfeldt, Daniel Rolles, Henry N. Chapman, and Jochen Küpper, “Toward atomic resolution diffractive imaging of isolated molecules with x-ray free-electron lasers,” *Faraday Disc.* **171**, 393 (2014), arXiv:1403.2553 [physics].
- [24] Salah Awel, Richard A. Kirian, Max Wiedorn, Kenneth R. Beyerlein, Nils Roth, Daniel A. Horke, Dominik Oberthür, Juraj Knoska, Verlerio Mariani, Andrew Morgan, Luigi Adriano, Alexandra Tolstikova, Paulraj Lourdu Xavier, Oleksandr Yefanov, Andrew Aquila, Anton Barton, Shatabadi R. Chowdhury, Mark S. Hunter, Daniel James, J. Robinson, Uwe Weierstall, Andrei V. Rode, Jochen Küpper, and Henry N. Chapman, “Femtosecond x-ray diffraction from an aerosolized beam of protein nanocrystals,” (2016), in preparation.
- [25] G. Golovin, S. Banerjee, J. Zhang, S. Chen, C. Liu, B. Zhao, J. Mills, K. Brown, C. Petersen, and D. Umstadter, “Tomographic imaging of nonsymmetric multi-component tailored supersonic flows from structured gas nozzles,” *Appl. Opt.* **54**, 3491 (2015).
- [26] Björn Landgraf, Michael Schnell, Alexander Sävert, Malte C. Kaluza, and Christian Spielmann, “High resolution 3d gas-jet characterization,” *Rev. Sci. Instrum.* **82**, 083106 (2011).
- [27] L. Strüder, Sascha Epp, Daniel Rolles, Robert Hartmann, Peter Holl, Gerhard Lutz, Heike Soltau, Rouven Eckart, Christian Reich, Klaus Heinzinger, Christian Thamm, Artem Rudenko, Faton Krasniqi, K. Kühnel, Christian Bauer, Claus-Dieter Schroeter, Robert Moshammer, Simone Techert, Danilo Miessner, Matteo Porro,

Olaf Haelker, Norbert Meidinger, Nils Kimmel, Robert Andritschke, Florian Schopper, Georg Weidenspointner, Alexander Ziegler, Daniel Pietschner, Sven Herrmann, Ullrich Pietsch, Albert Walenta, Wolfram Leitenberger, Christoph Bostedt, Thomas Moeller, Daniela Rupp, Marcus Adolph, Heinz Graafsma, Helmut Hirsemann, Klaus Gaertner, Rainer Richter, Lutz Foucar, Robert L Shoeman, Ilme Schlichting, and Joachim Ullrich, “Large-

format, high-speed, x-ray pnccds combined with electron and ion imaging spectrometers in a multipurpose chamber for experiments at 4th generation light sources,” *Nucl. Instrum. Meth. A* **614**, 483–496 (2010).

- [28] Yuan-Pin Chang, Daniel A. Horke, Sebastian Trippel, and Jochen Küpper, “Spatially-controlled complex molecules and their applications,” *Int. Rev. Phys. Chem.* **34**, 557–590 (2015), arXiv:1505.05632 [physics].